On Forcings of Length of Day Changes: from 9-day to 18.6-year oscillations

J.L. Le Mouël, F. Lopes, V. Courtillot and D. Gibert (Rev2-16/04/19)

Geomagnetism and Paleomagnetism, Institut de Physique du Globe de Paris, 1 rue Jussieu, Paris, France

Corresponding author: Vincent Courtillot (courtil@ipgp.fr)

Abstract

We analyze fluctuations in Earth's rotation velocity (therefore also the equivalent length of day), using more than 50 years of IERS observations and the powerful method of Singular Spectral Analysis. The first 16 eigenvalues uncovered by SSA correspond to 10 components, all with physical sense. The first component is the trend, the second is the lunar node tide (18.6 yr, amplitude 1.3 ms). Next are variations with a period that implies forcing related to solar activity (11 years, 0.46 ms amplitude). Then, zonal oscillations linked to the solar (1 year, 0.81 ms; 0.5 year, 0.76 ms;) and lunar (27.54 days, 0.39 ms; 13.66 days, 0.73 ms; 13.63 days, 0.27 ms; 9.13 days, 0.14 ms) tidal potentials. The QBO at 2.36 years (0.08 ms) is interpreted as a Sun-related oscillation. The components at 13.63 and 13.66 days could contain a solar contribution. SSA is an efficient detrending algorithm and way to identify irregular (quasi-periodical) oscillatory components: its application to l.o.d. data yields refined observations, in good agreement with recent models but with some new results. There is no extracted component that could not be attributed to an existing periodic or quasi-periodic physical phenomenon. Progress in computers and signal processing have allowed us to resume and extend the analysis of l.o.d., and in particular to show evidence of a solar signature in the series. Uncovering the mechanisms through which solar activity acts on Earth's rotation is an exciting project for geophysicists that deserves renewed attention.

1 – Introduction

It has been known for decades that the Earth's rotation velocity (or the associated changes in length of the day l.o.d.) presents irregularities on different time scales (e.g. Guinot, 1973; Lambeck, 2005). Various fluctuations, some irregular, others pseudo-periodical, with time constants from a few days to a few decades, are superimposed on a quasi-linear trend. This long-term deceleration is due to a braking of the Earth's rotation by tidal forces. Its rate is well-known from the study of the Earth-Moon system and is of the order of 2 ms per century.

We focus in this paper on the l.o.d. time series from 1962 to 2018, a time span of a little more than a half century. In Figure 1 (top) the “l.o.d data” consist in five-day averages of length of the day from the International Earth Rotation Service (IERS, Paris, France), (Lambeck, 2005; see e.g. Jault and Le Mouël, 1991, for an illustration).

The spectrum of the series can be split into three parts (Figure 1 bottom): lower-frequency harmonic oscillations, oscillations linked to zonal solar (6 and 12 months) and lunar (27.54 days and harmonics) tides, and irregular variations in the range of a few days to a few decades. The lower-frequency variations have been attributed mainly to an exchange of angular momentum between the mantle and the core of the Earth: there is no angular momentum sink in the atmosphere that is large enough to account for it (e.g. Hide, 1977). In this paper, we focus on possible external causes (external to the solid Earth) of the variations of l.o.d. with time scales longer than a few days up to a few decades.

Lambeck (1980) noted in an analysis of changes of l.o.d. and atmospheric circulation that "a relation between solar activity and the Earth's rotation cannot be dismissed". Currie (1980) identified an 11-yr component using maximum entropy spectral analysis. In Le Mouël et al (2010), we studied the evolution of the amplitude of the seasonal semi-annual variation of l.o.d. from 1962 to 2009; we focused on the detection of the 6-month (and 12-month) spectral lines. The former was indeed found to be modulated in amplitude with 11-yr quasi-periodicity. We had already found some evidence of the influence of solar activity on l.o.d. in Le Mouël et al (2004). With the method used in Le Mouël et al (2010), we did not conclude on the nature of this modulation effect. Using augmented data and the Singular Spectrum Analysis (SSA) method, we identify in this paper spectral components of l.o.d. that can be connected to lunar and solar tidal effects and also to variations in solar activity. We determine rather precisely the periods and also the amplitudes of these components. These new observations will be compared to a recent model of the long-period tidal variations in lod (Ray and Erofeeva, 2014).

2 –The SSA method of analysis

Singular-spectrum analysis (SSA) is a powerful method of spectral analysis that works well with short and noisy time series. We refer the reader to the detailed monograph by Golyandina et al [2001]. Useful accounts are found in Vautard and Ghil [1989], Ghil et al. [2002] and Vautard et al. [1992]. Some remarks that may help readers unfamiliar with SSA are given in Appendix 2. Many geophysical time series are "short" in a numerical sense, i.e. their length is not very much longer than some of the periodicities that they might contain. Moreover, they actually often contain pseudo-periodicities that fluctuate in both amplitude and pseudo-period. SSA provides at the same time a noise reduction technique, a detrending algorithm and a way to identify oscillatory components. SSA has been applied to the irregular ENSO phenomenon, to global-surface temperature, to geopotential height data, to a number of indicators of climate variability, to solar observations, and to cosmogenic isotopes. Lopes et al. [2017] isolated pseudo-periodic 11 and 5.5- year variations in a century-long series of rotation pole positions of the Earth's mantle.

In this paper, we perform singular spectrum analysis of IERS l.o.d. series that confirms some older results and brings out several new ones. We refer the reader to Lopes et al. [2017] for more information on the way in which we use the method. In Appendix 2 we briefly explain why our method is able to produce some original results~~, not noted before as far as we know.~~

3 – Results of the SSA analysis

We show the magnitude of eigenvalues of the l.o.d. time series in decreasing order of amplitude in Figure 2 (amplitude is peak to peak in ms). Most of the first 16 eigenvalues, corresponding to 10 components (6 consist in pairs of similar eigenvalues), can be assigned to a physically meaningful source: their frequencies or pseudo-frequencies can be found either in the rotation of the Moon around the Earth, of the Earth around the Sun, or in solar rotation and variations in solar activity. They are ranked in the order of decreasing amplitude of eigenvalues or pairs of eigenvalues: first the trend, then periods of 18.6 years, 1 year, 11.5 years, 0.5 year, 13.66 days, 27.54 days, 13.63 days, 9.13 days and 2.36 years.

Figure 3 top shows the first component (corresponding to the first eigenvalue) extracted by SSA, which is the trend of the series. It comprises the long-term (secular) decrease in l.o.d. and multi-decadal oscillations. The spectrum of SSA component 1 is almost identical to that

of the full series for periods longer than 5 years (Figure 3 bottom vs 1 bottom). We next present the results of the rest of the analysis: longer period variations with a clear solar origin, intermediate period zonal tidal effects of the Moon and Sun, and QBO variations. Further interpretation of these results is discussed in section 4.

Let us first recall the frequencies that could be expected from astronomical and astrophysical forcings by the Sun and Moon. In previous papers, we have analyzed a number of solar proxies, including sunspot number ISSN and number of polar faculae PF, using SSA and Fourier analysis (e.g. Le Mouël et al. [2018]). The sunspot cycle and its harmonics are often the prominent components at 11, 5.5 and 3.6 years; also prominent are the solar zonal tidal annual and semi-annual lines. For the Moon, tidal zonal contributions are expected at the lunar month period (27.54 days) and its harmonics (13.77, 9.18,...). Finally, one might expect to find the solar synodic rotation at 27.27 days and its harmonics (13.63, 9.09,...).

The first seven components of a recent l.o.d model (Ray and Erofeeva, 2014) are listed in the second column of Table 1. They are the main components of a model that comprises 80 spectral lines and includes, in addition to the elastic responses the effects of mantle anelasticity and dynamic ocean tides. They range from the 18.6 lunar node tide, through the Sa (365.25 days), Ssa (182.62 days), Mm (27.55 days), Mf (13.66 and 13.63 days), and Mt (9.13 days) to 4.7 days.

We stress that this is a model made to fit with a number of parameters the then observed spectral lines of l.o.d. Here we analyze with SSA an augmented set of data leading to improved spectral resolution. The values of the main SSA components that we calculate are listed in the next to last column of Table 1 and discussed briefly below.

Following the trend, second only to it in amplitude, we find a component at the lunar node tide period of 18.6 years (Figure 4, component 2, amplitude 1.3 ms - note: all amplitudes are peak to peak). We briefly explain in Appendix 2 that this component is not extracted exactly in the same way as all the following ones). To our knowledge, this large nutation had been predicted by models (Ray and Erofeeva, 2014) but not observed before.

3.1 –Longer period (solar activity) variations

We next find the 11-yr solar cycle, the so-called Schwabe cycle, with an amplitude of 0.46 ms (Figure 5 top; component 4). Its period is 11.5 ± 2.5 yr (we adopt as an estimate of uncertainty on period the “half-line” width at half ordinate value of the peak - Figure 5 bottom). In pioneer work, Currie (1980) had identified an 11-yr oscillation in l.o.d. (with an

amplitude of 0.16 ms) using Maximum Entropy Spectral Analysis. We identified earlier this oscillation in the series of mantle rotation pole positions (Lopes et al., 2017). Note that, on the available time span, we have only five 11-yr oscillations, one being incomplete. The main period of the component is close to 12 years (Figure 5 bottom). Recall that individual solar cycles may last from 9 to 14 years. In solar proxies, we find significant harmonics at about 5.5 and 3.6 years (Le Mouël et al., 2018), but not in the l.o.d. analysis (at least not among the first 16 eigenvalues).

3.2 –Zonal solar and lunar tide oscillations

SSA also provides us with a new estimate of components of l.o.d. variations whose existence has been known for long, i.e. the annual and semi-annual lines (Figures 1 bottom, 6 and 7). Note that the method provides the singular oscillations themselves, rather than global spectral properties corresponding to more or less long intervals (Figures 6 and 7; components 3 and 5; respective amplitudes of 0.81 and 0.76 ms). The stability of the seasonal amplitudes and phases is quite remarkable for both the annual and semi-annual variations. Nevertheless, a small increase of the annual oscillation amplitude from 1962 to the late 1980s is accompanied by a small decrease of the semi-annual one. These oscillations can logically be attributed to the zonal parts of the solar gravitational/tidal potential. In the shorter-period interval, SSA isolates quasi-sinusoidal variations with periods 13.66 days (Figure 8 bottom; component 6, amplitude 0.73 ms), 27.54 days (Figure 9 bottom; component 7, amplitude 0.39 ms), 13.63 days (Figure 10 bottom; component 8, amplitude 0.27 ms) and 9.13 days (Figure 11 bottom; component 9, amplitude 0.14 ms). These oscillations could be due to the zonal parts of the lunar gravitational/tidal potential: one component is at the lunar month period of 27.54 days; the 13.66 and 13.63 day components (the precision of our determinations is such that these values can actually be considered as distinct; we will see a complementary interpretation in section 4) are close to its first harmonic at 27.54/2 = 13.77 days and the 9.13 day component to the second harmonic at 27.54/3 = 9.18 days.

3.3 – A QBO (quasi biennal oscillation)

Finally, SSA analysis provides us with a small amplitude but clear quasi-biennial oscillation (Figure 12 top; component 10; amplitude 0.08 ms) in l.o.d.: its period is 2.36 years or about 28 months. In their review paper, Baldwin et al. (2001) recall that "the QBO dominates the variability of the equatorial stratosphere and is easily seen as downward

propagating easterly and westerly wind regimes, with a variable period averaging approximately 28 months". We can therefore certainly call component 10 in Figure 12 top a QBO. Its amplitude of 0.08 ms is modulated in the available time span by a longer wavelength variation whose pseudo-period (if there is one) cannot be estimated on this too-short time-scale (but larger than 60 years). Component 10 is the only significant QBO oscillation that we have detected in the l.o.d. series.

4 – Discussion

We start the discussion by first giving a few elementary relationships that are useful in the following. Our observation ("observable") is the length of the day. The mean *lod* is $\tau =$ 86,400 s and in the calculations below, we use $\tau = 0.86\ 10^5$ s; the corresponding mean rotation rate of the solid Earth is $\omega_M = 7.3 \times 10^{-5}\ \mathrm{rad \cdot s^{-1}}$. The relationship between the change in rotation rate and the change in l.o.d. is:

$$\delta\omega_M = \frac{-2\pi}{(lod)^2}\delta lod = -\ 8.5 \times 10^{-10}\delta lod \qquad (1)$$

4.1 – Solar generated oscillations

We *observe* variations in the length of day with periods that are characteristic of solar activity. We attribute them, rather naturally, to solar action on planet Earth, in the form of a torque Γ_S with period $T = 11$ yr (Schwabe). The 13.63 and 13.66-day components are close to the first harmonic of the solar synodic rotation period 27.27/2 = 13.63 days (but see below). Direct influence of solar activity on the solid Earth - with its magnetic field - is generally considered too weak (e.g. see discussion in Currie, 1980, or references in Lopes et al., 2017). This leads us to consider a simple model, in which the solar torque acts on the atmosphere (see also e.g. Gray et al, 2010; Forbes, 2000). As for the coupling of the lower atmosphere and the Earth's surface, we refer the reader to, e.g., Smith (1979).

Let $\Gamma_S^T = \gamma_T\ exp(2i\pi t/T)$; the axial moment of inertia of the solid mantle is $I_M = 7.\ 10^{37}$ kg.m^2. The component of its axial angular momentum with period T due to Γ_S^T is $I_M\ \delta\omega_M^T\ exp(2i\pi t/T)$. The corresponding value of the atmospheric variation of angular momentum is $I_A\ \delta\omega_A^T\ exp(2i\pi t/T)$; ω_A^T is the equivalent angular rotation momentum of the atmosphere, that can in principle be calculated from the azimuthal wind field u_ϕ. The mantle and atmosphere are linked by a torque $\Gamma = k(\delta\omega_M^T - \delta\omega_A^T)$, where k is a friction coefficient. Dropping the exponential factor and introducing the frequency $u=2\pi/T$, we obtain the following equations:

$$iu\,(I_M\,\delta\omega_M) = \Gamma = k\,(\delta\omega_M - \delta\omega_A) \qquad (2)$$

$$iu\,(I_M\,\delta\omega_M + I_A\,\delta\omega_A) = \Gamma_S$$

The discussion of equation (2) is simple: when k -> 0, $\delta\omega_M$ -> 0. The mantle does not rotate and $\delta\omega_A = \Gamma_S / iu\,I_A$. When k -> ∞ , the mantle and atmosphere rotate rigidly together. It may be useful to give an order of magnitude of the coupling torque Γ. For example, for the 11-yr oscillation, $\Gamma_M^{11} = \gamma_M^{11}\,exp(2i\pi t/T)$ and $\gamma_M^{11} = I_M\,\delta\omega_M^{11}\,u = 7.10^{37}\ 8.510^{-10}\ 46.10^{-5}\ 2\pi/11.\pi.10^7 = 4.97\ 10^{17}$ kgm^{2}s^{-2}, using the *observation* $\delta lod^{11} \sim 0.46$ ms (Figure 5).

We recall that the only data (observable) we have recourse to is ω_M^T for some long-period variations of ω_M. An estimate of ω_A (or the equivalent zonal velocity u_ϕ) requires the knowledge of Γ_S, the solar torque. For an estimate of Γ_S, we could appeal to two mechanisms. Either the UV and extreme UV solar radiations, that have large relative variations up to 10% during a solar cycle (contrary to total solar irradiance that varies by only 0.1%). Or the solar wind, that is also known to vary significantly during a solar cycle as shown for instance by the variations in the count of faculae (e.g. Blanter et al, 2018). Some efforts have been devoted to evaluating the action of solar activity on the atmosphere, most often of the ionized atmosphere. But to our knowledge, there is as yet no available estimate of Γ_S. And as long as we do not know it better, we cannot evaluate ω_A (or the equivalent zonal velocity u_ϕ) through equation 2, though we could propose a range of estimates. We do not pursue this topic in the present paper.

4.2 – Zonal tidal oscillations

The first idea that comes to one's mind is that all the components in section 3.2 are due to zonal tides, related to the Sun for components 2 and 4, and to the Moon for components 6 to 9. In Appendix 1, we give a simplified version of the well-known theory of these tides and their effect on l.o.d. This allows us to compare the main components of l.o.d. variations that we have detected in the l.o.d. series using SSA with the values generated by the simple model in Appendix 1. The results are listed in the last column of Table 1. The Love number κ that best fits the amplitudes we observe is 0.309.

We find an excellent agreement (between 2% and 5%) between the observations and the values provided by the model for the annual Sa and semi-annual Ssa periods, as well as the lunar monthly period Mm (27.54 days). But there is a discrepancy of a factor five between the observed and the model amplitudes of the 13.66-day component. Furthermore, this amplitude

is twice as large as the amplitude of the fundamental lunar period of 27.54 days, which is not expected for an harmonic. And we must account for the component at 13.63 days. Thanks to the high-density sampling of the l.o.d. series, the 13.66 and 13.63 periods can be significantly separated. The 13.63-day period is on first analysis not a lunar harmonic (27.54/2 = 13.77), and 13.63 is half of the 27.27-day period of the Sun's synodic rotation period. We propose that the 13.66 component with its "anomalous" amplitude, and the 13.63 component, that is 27.27/2, could (at least in part) be solar generated. Unfortunately, no realistic model of solar activity action on Earth (that is torque) is available. The 9.13-day period on the other hand is expected to be generated by lunar zonal tides.

In Table 1, we can also compare the amplitudes of the lines/components/eigenvalues that are predicted by Ray and Erofeeva's (2014) model and our observations derived directly from the l.o.d. data using SSA. The amplitudes of the 27.54, 13.66, 13.63 day lines are in excellent agreement (from 1 to 10% discrepancy). On the other hand, the lunar node tide, annual and semi-annual line amplitudes are respectively stronger by a factor on the order of 4, 16 and 2.

4.3 – QBO oscillations

Quasi-biennial oscillations have been observed in the variations of different geophysical parameters: e.g. near-surface temperature, SAT and NAO indices (Palus and Novotna, 2008), and stratospheric winds (Baldwin et al, 2001). The (pseudo) period of these oscillations is distributed in a rather large time interval; 1.6 to 1.9-year oscillations found by Menvielle and Marchodon (2007) in sudden storm commencements (ssc) for solar cycles 11 to 22, and those found by Valdes-Galicia et al. (1996) and Kato et al. (2003) in cosmic rays in the outer heliosphere have similar periods. And an approximate one-to-one correspondence is found between oscillations in ζ ratios and cosmic rays in the 1982-1992 time span – the only one available (Figures 3 and 5 of Kato et al, 2003).

A complete analysis of the ISSN data shows a component at 2.36 years, which is the fourth harmonic of the Schwabe cycle (2.36 x 5 = 11.8) (Figure 13). We suggest that the 2.36 year QBO SSA component in l.o.d. could be yet another solar signature.

Baldwin et al (2001) noted that alternating wind regimes repeat at intervals that vary from 22 to 34 months (1.8 to 2.8 years). At the time of their review, these authors commented that "whether or not decadal variability (*in QBO*) is caused by the 11-year solar cycle ... there is increasing evidence through modeling that the solar cycle has a significant influence on

winds and temperatures in the upper stratosphere". They concluded that "circulation changes introduced in the stratosphere penetrate downward, even reaching the troposphere." The QBO signal was first identified in the l.o.d. series by Lambeck and Cazenave (1973), as a peak in its Fourier transform. We confirm and improve significantly its description by our SSA observations (Figure 13).

5 – Conclusion

We have analyzed in this paper fluctuations in Earth's rotation velocity, or equivalently length of day, using more than 50 years of IERS data and the powerful method of Singular Spectral Analysis. The first 16 eigenvalues uncovered by SSA correspond to 10 components, all with physical sense. The first component is simply the trend, followed by the lunar node tide period (18.6 yr, amplitude 1.3 ms). Next, we observe variations with a period that implies forcing related to solar activity (11 years, 0.46 ms amplitude; QBO at 2.36 year, 0.08 ms)); then, zonal oscillations linked to the solar (1 year, 0.81 ms; 0.5 year, 0.76 ms) and lunar (27.54 days, 0.39 ms; 9.13 days, 0.14 ms) tidal potentials. A doublet at periods 13.66 days (0.73 ms) and 13.63 days (0.27 ms) warrants further discussion. These periods are predicted by the model of Ray and Erofeeva (2014) with approximately correct amplitudes. But these are fits to earlier data with seven adjustable parameters; in that model this doublet which is close to the fortnight lunar tide Mf is considered to be lunar. We have seen that the period values and the line amplitudes are not what would be expected for a lunar harmonic. We suggest that at least part of these components could be solar related.

Because SSA is at the same time an efficient noise reduction technique, detrending algorithm and way to identify irregular (quasi-periodical) oscillatory components, its application to l.o.d. data has yielded some updated and some new results. The trend includes the long term lunar tidal braking and possibly solar components with a longer time scale than can be identified with only a half century of observations (e.g. the Gleissberg and de Vries pseudo-periods). Then we identify the lunar node tidal period that was predicted but to our knowledge not yet observed. The 11-yr component is of course forced by the Sun and its changes in activity. The lunar monthly tide is clearly isolated but, more interestingly, it can be argued that the two prominent components at 13.66 and 13.63 days are at least in part solar components. And finally, we propose that the QBO at 2.36 years is actually generated by solar activity. In conclusion, there is no line that cannot be attributed to an existing quasi-

periodic physical phenomenon. And again all the SSA eigenvalues we determine here are essentially updated, refined *observations*, not the results of a *model*.

Careful study of the Earth's rotation, in particular of the length of the day (the "axial" problem) is what geoscientists call "a secular problem". Progress in computers and signal processing have allowed us to resume and extend the analysis of l.o.d., and in particular to show evidence of a solar effect in the series, that we had discovered in the motion of the pole and discussed more succinctly (the "equatorial" problem). Uncovering the mechanism through which solar activity acts on Earth's rotation and on a number of climatic indices is an exciting project for geoscientists that deserves renewed attention (Le Mouël et al. [2018]).

Appendix 1: Effect of solar and lunar zonal tides on the Earth's rotation

It is sufficient an approximation for our purpose to suppose that the Earth, when not submitted to the action of external forces, is a sphere of radius a. The cases of the Sun and Moon gravitational potentials can be treated in the same way. Let us start with the zonal part of the Sun's potential at a point with latitude θ at the Earth's surface (Jobert, 1973; Guinot, 1973; Lambeck, 2005):

$$U_2 = G\,M\,a^2\,D^{-3}\,P_2(\sin\theta)\,P_2(\sin\delta) \qquad \text{(A1-1)}$$

where G is Newton's constant, M the mass of the Sun, $\delta(t)$ its declination, a the Earth's radius, $D(t)$ the Sun-Earth distance and P_2 the Legendre polynomial of degree 2 ($P_2(\sin\delta)=(3\sin^2\delta-1)/2$). The same applies to the Moon with the relevant values of M, D and δ. For the Sun, the term $G\,M\,a^2\,D^{-3}$ contains mainly an annual period through D, and the term $P_2(\sin\delta)$ a semi-annual period. For the Moon the corresponding periods are the lunar month (~ 28 days) and a semi-monthly period (~14 days).

The spherical Earth is considered to be elastic and submitted to the perturbating potential U_2. The resulting deformation of the Earth creates an additional potential V_2, also of degree 2, and from the theory of Love at the Earth's surface $V_2 = \kappa\,U_2\,(r=a)$. κ is the Love number (e.g. Jobert, 1973; Lambeck, 2005). Let $O\,x_1\,x_2\,x_3$ be a system of axes linked to the Earth (Ox_3 is the axial axis), x_1, x_2 and x_3 being the coordinates of the current point of observation exterior to the Earth ($r = \sqrt{(x_1^2+x_2^2+x_3^2)} > a$). In the absence of U_2, the Earth's moments of inertia are equal. We are dealing with an axisymmetric problem, and the expression of V_2 is easily obtained as a function of the additional moments of inertia c_{ii}

resulting from the perturbation (c_{ij}=0 i≠j; c_{22}=c_{11}):

$$V_2(r) = (G/2r^5)(c_{33} - c_{11})\,(x_1^2+x_2^2-2x_3^2) \qquad \text{(A1-2)}$$

Furthermore, if the deformation follows the Love hypothesis, $\Sigma c_{ii} = 0$ and $c_{33} - c_{11} = (3/2)\,c_{33}$. The function $(x_1^2+x_2^2-2x_3^2)/\,r^5$ is harmonic and, using spherical coordinates θ (colatitude) and r=a:

$$V_2(a,\theta) = (3G/4a^3)\,c_{33}\,(1/3 - \sin^2\theta) = kU_2(a) \qquad \text{(A1-3)}$$

U_2 being given by equation (1); one obtains:

$$c_{33} = k\,M\,a^5 D^{-3}(t)\,(1/3 - \sin^2\delta(t)) \qquad \text{(A1-4)}$$

One still has to relate the variation of the Earth's axial rotation m_3, with $\Omega(t) = \Omega_0\,(1 + m_3(t))$, $\Omega_0 \sim 7.26\ 10^{-5}$ rad/s. The third equation of the Euler system gives $m_3 = -\,c_{33}/I_M$ where I_M is the axial moment of inertia of the mantle ~7. 10^{37} kg.m^2; the variations of the Earth's spin rate are $m_3(t)\Omega_0$.

$D(t)$ and $\delta(t)$ are found in catalogs. We are especially interested in the amplitudes of the annual and semi-annual oscillations for the Sun, and of the lunar month and semi-lunar month for the Moon's oscillations. We find that a value of the Love number κ=0.309 best fits the theoretical amplitudes to the ones we actually observe.

Appendix 2: Some remarks on the use of SSA

We propose here some remarks that briefly describe the main features of SSA and some of the ways we apply it. References to several books and papers are given in the main text and in this appendix. Vautard and Ghil (1981) combine and generalize the theory of spectral decomposition, as unified by Karhunen (1946) and Loève (1946), with the embedding theorem of Mane (1981) and Takens (1981).

The first theory initiated by Karl Weierstrass in 1958 consists in proving the existence of decomposition bases that are favored when one diagonalizes symmetric matrices that describe certain endomorphisms : in the case of l.o.d., can we decompose the series on a basis of orthogonal sub-systems that, taken independently one from the other, would allow a better understanding of the complexities of the problem?

A second theory deals with the best possible way to build the symmetric matrix, diagonal matrices being a particular case, without losing information from the starting series. Once the linear system is built, one has only to extract the families of eigenvectors and eigenvalues needed to reconstruct the signal. For this, one uses the SVD (Singular Value

Decomposition; Golub and van Loan, 1980) algorithm to decompose the signal on an orthogonal basis.

The main difficulty is the proper construction of the symmetrical matrix. For Vautard et Ghil (1981), using a Toeplitz matrix with constant sampling interval is the main characteristic of such a decomposition, but this is still a debated question, and other families of symmetric matrices are used by different scientific communities. In their chapters 1 and 6, Golyandina et al (2001) review this topic. Practically, this matrix is not very different from the autocorrelation matrix of the signal, in which each column is a segment of length L of the starting time series. The size L of this window constrains the periods that can be extracted. In the case of the l.o.d. series analyzed in this paper, we have extracted relatively short periods with L = 5000 points, whereas for the lunar node tide with period 18.6 years, we have had to use 15,000 points. We can therefore sum up all components extracted with L = 5000, but we cannot add the lunar node component obtained with a different L, for the reason that part of the energy of shorter periods can already be included in that component. The unicity of decompositions is valid for a given L, not for a set of different L values.

The next question is the proper choice of L. This is not a trivial problem and the method remains widely discussed (Golyandina et al., 2001, chapter 6.1). In principle, perfect separability of components for any L requires that, in the U and V matrices of eigenvectors obtained by SVD of the l.o.d. diagonal matrix, the i^{th} column of U be exactly orthogonal to the i^{th} line of V. Such is of course never the case and this is why new algorithms are proposed such as VARIMAX for the eigenvectors or decentered SVD, in order to be as close as possible to the orthogonality condition (Golyandina et al., 2001). Another more practical method is to apply SSA to a range of close-by values of L rather than a single one and to check the stability of the decomposition. This method has the advantage of allowing one to estimate the uncertainties in our reconstructed periods and amplitudes.

One must identify the families of eigenvectors and eigenvalues that correspond to one component. The autocorrelation matrix that one diagonalizes is simply giving autocorrelations of segments of the data; the most important or stable components (as is the case for a Fourier transform) or the strongest (in terms of amplitudes) have the larger eigenvalues. One only has to regroup eigenvectors that have equal (or very close) eigenvalues (see Figure 2).

In the way we use SSA, we use large computer power. The Hankel matrix we calculate has 1000x19,470 terms. We work with 64bit computers, and double precision numerics of 8bit each. SVD of that matrix yields two eigenvector matrices and one matrix with

eigenvalues that have the same dimensions. We therefore require an 8Go active memory, which means we must run on a computer with at least 10Go. This is what we do and one reason why we obtain the new results presented in this paper. This is also why we do not need to apply a Monte Carlo SSA algorithm, which is in a way a bootstrap method that must be used (implying loss of information) only when the computer that is used is not powerful enough.

Acknowledgements:

We thank the editor for help and suggestions, and reviewer Kurt Lambeck for comments that led to considerable improvement of the original version of this paper. IPGP Contribution xxx.

References:

Baldwin, M.P. and 14 co-authors, The quasi-biennal oscillation, *Rev. Geophys.*, **39** (2), 179-229, paper number 1999RG00007, 2001.

Blanter, E., Le Mouël, J.L., Shnirman, M., and Courtillot, V., Long Term Evolution of Solar Meridional Circulation and Phase Synchronization Viewed Through a Symmetrical Kuramoto Model , *Solar Phys.*, 293:134 doi.org/10.1007/s11207-018-1355-9, 2018.

Defraigne, P., and Smits, I., Length of day variations due to zonal tides for an inelastic earth in non-hydrostatic equilibrium, *Geophys. J. Int.*, **139**, 563-572, 1999.

Currie, R.G., Detection of the 11-yr sunspot cycle signal in Earth rotation, *Geophys. J. Roy. Astr. Soc.*, **61**, 131-140, 1980.

Forbes, J.M., Wave coupling between the lower and upper atmosphere: case study of an ultra-fast Kelvin wave. *J. Atmos. Sol. Terr. Phy.* **62** (17), 1603–1621, 2000.

Ghil, M., and 10 co-authors, Advanced spectral methods for climatic time series, *Rev. Geophys.*, **40** (1), 1003, doi: 10.1029/RG000092, 2002.

Golub, G. H. and van Loan, C. F., An analysis of the total least squares problem, *SIAM Journal of Numerical Analysis*, **17**(6), 883-893, 1980.

Golyandina, N., Nekrutkin, V., Zhigljasky, A. (2001), *Analysis of Time Series Structure: SSA and related techniques*, Monographs on Statistics and Applied Probability 90, Chapman and Hall, Boca Raton, 295pp.

Gray, L.J., Beer, J., Geller, M., Haigh, J.D., Lockwood, M., Matthes, K., Cubasch, U., Fleitmann, D., Harrison, G., Hood, L., et al., Solar influences on climate, *Rev. Geophys.* **48** (4), 2010.

Guinot, B., Variation du pôle et de la vitesse de rotation de la Terre, ch. 19, in *Traité de Géophysique Interne*, vol. 1, J. Coulomb and G. Jobert eds., Masson, Paris, France, 529-564, 1973.

Hide, R., Experiments with rotating fluids, *Quarterly Journal of the Royal Meteorological Society,* **103(435)**, 1-28, 1977.

Jault, D., and Le Mouël, J.L., Exchange of Angular Momentum between the Core and the Mantle , *J. Geomag. Geoelectr.*, **43**, 111-129, 1991.

Jobert, G., Marées terrestres, ch. 18, in *Traité de Géophysique Interne*, vol. 1, J. Coulomb and G. Jobert eds., Masson, Paris, France, 507-527, 1973.

Karhunen, K., Zur spektraltheorie stochastischer prozesse, *Ann. Acad. Sci. Fennicae*, AI, 34, 1946.

Kato, C., Munakata, K., Yasue, S., Inoue, K., and McDonald, F.B., A 1.7-year quasi-periodicity in cosmic ray intensity variation observed in the outer heliosphere, *J. Geophys. Res.*, **10**, 1367, doi:10.1029/2003JA009897, 2003.

Lambeck, K., Changes in length of day and atmospheric circulation, *Nature*, **286**, 104-105, 1980.

Lambeck, K., *The Earth's Variable Rotation: Geophysical Causes and Consequences*, Cambridge University Press, 2005.

Lambeck, K., and Cazenave, A., The Earth's rotation and atmospheric circulation—I Seasonal variations, *Geophysical Journal International*, **32**, 79-93, 1973.

Le Mouël, J.L., Blanter, E.M., Chulliat, A., and Schnirman, M., On the semiannual and annual variations of geomagnetic activity and components, *Ann. Geophys. (1983),* **22**, 3583 – 3588, 2004.

Le Mouël, J.-L., Blanter, E., Shnirman, M., and Courtillot, V., Solar forcing of the semi-annual variation of length-of-day, *Geophys. Res. Lett.*, **37**, L15307, doi:10.1029/2010GL043185, 2010.

Le Mouël, J.L., Lopes, F., and Courtillot, V., A Solar signature in several climatic indices, *J. Geophys. Res.,* 2018, submitted.

Loève, Michel, Fonctions aléatoires de second ordre, *Revue science*, **84**, 195-206, 1946.

Lopes, F., Le Mouël, J.L., Gibert, D., The mantle rotation pole position: A solar component, *C. R. Geoscience*, **349**, 159-164, 2017.

Mane, R., On the dimension of the compact invariant sets of certain non-linear maps, Springer, 230-242, 1981

Menvielle, M., Marchodon, A., Geomagnetic indices in solar-terrestrial physics and space weather, in: Lilensten, J., ed., Space Weather, Research towards applications in Europe, Astrophys. and Space Science Library, Springer , **344**, 277-288, 2007.

Palus, M., Novotna, D., Detecting Oscillations Hidden in Noise: Common Cycles in Atmospheric, Geomagnetic and Solar Data, Chapter in *Lecture Notes in Earth Sciences*, 26 pp., August 2008 DOI: 10.1007/978-3-540-78938-3_15

Ray, R. D., and S. Y. Erofeeva, Long-period tidal variations in the length of day, *J. Geophys. Res. Solid Earth*, **119**, 1498–1509, 2014, doi:10.1002/2013JB010830.

Smith, R.B., The influence of Mountains on the Atmosphere, *Advances in Geophysics*, **21**, 87-230, Academic Press,1979.

Takens, F., Detecting strange attractors in turbulence, Dynamical systems and turbulence, Springer, 366-381, 1981.

Temmer, M., Veronig, A., and Hanslmeier, A., Hemispheric Sunspot Numbers Rn and Rs: Catalogue and NS asymmetry analysis, *Astronomy & Astrophysics*, **390(2)**, 707-715, 2002.

Valdès-Galicia, J. F., Perez-Enriquez, R., and Otaola, JA., The cosmic-ray 1.68-year variation: a clue to understand the nature of the solar cycle?, *Solar Physics*, **167(1-2)**, 409-417, 1996.

Vautard, R. and Ghil, M., Singular spectrum analysis in nonlinear dynamics, with applications to paleoclimatic time series, *Physica D: Nonlinear Phenomena,* **35(3)**, 395-424, 1989.

Vautard, R., Yiou, P. and Ghil, M., Singular-spectrum analysis: A toolkit for short, noisy chaotic signals, *Physica D: Nonlinear Phenomena*, **58(1-4)**, 95-126, 1992.

Webb, D.F., Solar and geomagnetic disturbances during the declining phase of recent solar cycles, *Advances in Space Research*, **16(9)**, 57-69, 1995.

Table

Table 1: Amplitudes of components at given periods (1st column) as predicted by the Ray and Erofeeva (2014) model (column 2). Periods (column 3) and amplitudes (column 4) observed using SSA in this paper. Amplitudes calculated from the simple model in Appendix 1 of this paper (column 5).

Note: the amplitudes from the Ray and Erofeeva model are from their Table 3 columns 13 and 14 : Ampl = 2 $[\Delta\Lambda(\cos)^2+\Delta\Lambda(\sin)^2]^{1/2}$

Period - model (Ray-Erofeeva)	Amplitude - model (Ray-Erofeeva)	Period - observed (this paper)	Amplitude- observ (this paper)	Amplitude- model (this paper)
6798.40 days	159.86 μs 0.320 ms	6798.37 days	1.287 ms	
365.25 days	27.67 μs 0.055 ms	365.25 days	0.814 ms	0.7734 ms
182.62 days	173.49 μs 0.347 ms	182.62 days	0.760 ms	0.7298 ms
27.55 days	193.84 μs 0.388 ms	27.57 days	0.386 ms	0.3779 ms
13.66 days	359.42 μs 0.719 ms	13.66 days	0.730 ms	0.1388 ms
13.63 days	149.00 μs 0.298 ms	13.63 days	0.270 ms	
9.13 days	67.20 μs 0.134 ms	9.13 days	0.142 ms	

Figure legends

Figure 1: (top) Five-day averages of length of day (in ms) from Jan.1.1963 to Dec.31.2016, from International Earth Rotation Service. (bottom) Normalized spectrum of the time series above using FFT. Note the sharp 6-month and 1-year lines on the shorter period part of the figure.

Figure 2: The 30 first eigenvalues of the time series of l.o.d. in Figure 1a determined by Singular Spectrum Analysis (SSA) in decreasing order of magnitude (normalized). The components discussed in the text are identified (components correspond to either single eigenvalues or pairs of eigenvalues).

Figure 3: (top) The first SSA component of l.o.d. is the trend (in ms), as seen in Figure 1a. (bottom) Fourier transform (normalized spectrum) of the above (very similar to Figure 1b for periods larger than 5 years). A packet of energy is seen around 22 years.

Figure 4: (top) The second SSA component of l.o.d. at ~18.6 years (lunar node tidal period). (bottom) Fourier transform (normalized spectrum) of the above.

Figure 5: (top) The fourth SSA component of l.o.d. at ~11.5 years. (bottom) Fourier transform (normalized spectrum) of the above.

Figure 6: (top) The third SSA component of l.o.d. at 1 year. (bottom) Fourier transform (normalized spectrum) of the above.

Figure 7: (top) The fifth SSA component of l.o.d. at 0.5 year. (bottom) Fourier transform (normalized spectrum) of the above.

Figure 8: (top) The sixth SSA component of l.o.d. at 13.66 days. (bottom) Fourier transform (normalized spectrum) of the above.

Figure 9: (top) The seventh SSA component of l.o.d. at 27.54 days. (bottom) Fourier transform (normalized spectrum) of the above.

Figure 10: (top) The eighth SSA component of l.o.d. at 13.63 days. (bottom) Fourier transform (normalized spectrum) of the above.

Figure 11: (top) The ninth SSA component of l.o.d. at 9.13 days. (bottom) Fourier transform (normalized spectrum) of the above.

Figure 12: (top) The tenth SSA component of l.o.d. at 2.36 years (QBO). (bottom) Fourier transform (normalized spectrum) of the above.

Figure 13: (top) The 2.29 year component of ISSN superimposed on the tenth SSA component of l.o.d. at 2.36 years (QBO). (bottom) Fourier transform (normalized spectrum) of the above.

Figure 1

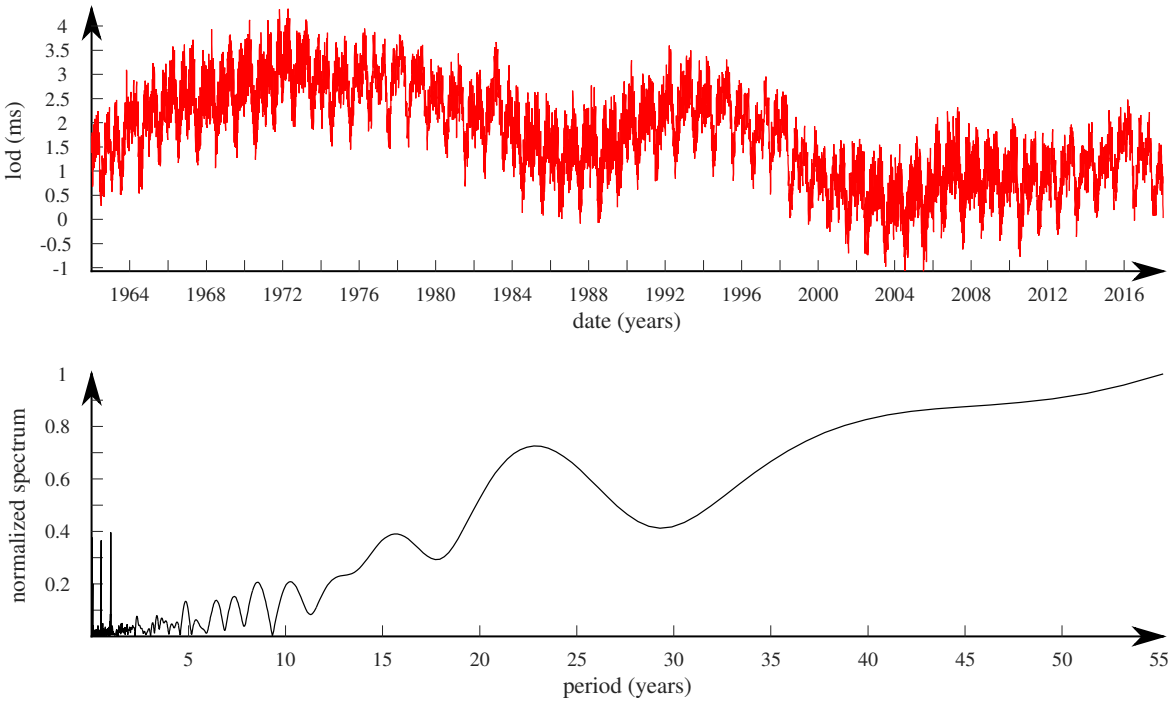
lod (ms)
4
3.5
3
2.5
2
1.5
1
0.5
0
-0.5
-1
1964
1968
1972
1976
1980
1984
1988
1992
1996
2000
2004
2008
2012
2016
date (years)
normalized spectrum
1
0.8
0.6
0.4
0.2
5
10
15
20
25
30
35
40
45
50
55
period (years)

Figure 2

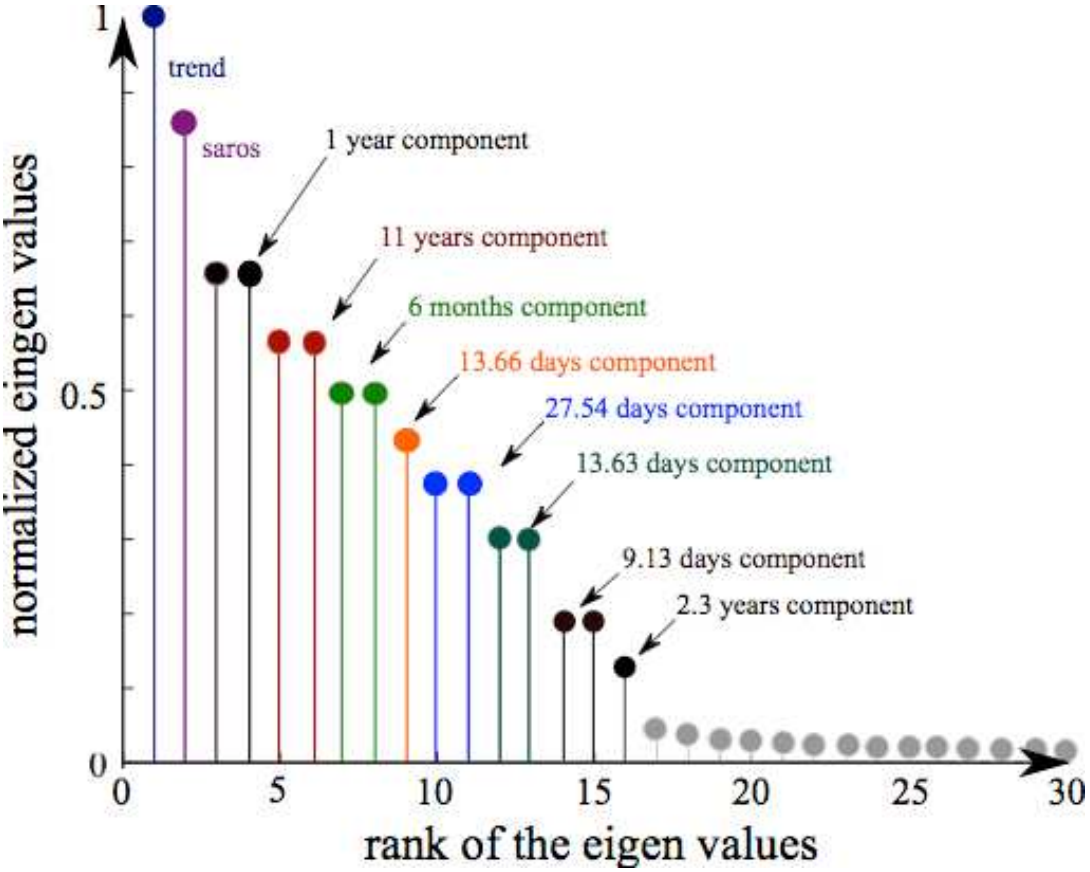
1
0.5
0
normalized eingen values
trend
saros
1 year component
11 years component
6 months component
13.66 days component
27.54 days component
13.63 days component
9.13 days component
2.3 years component
0
5
10
15
20
25
30
rank of the eigen values

Figure 3

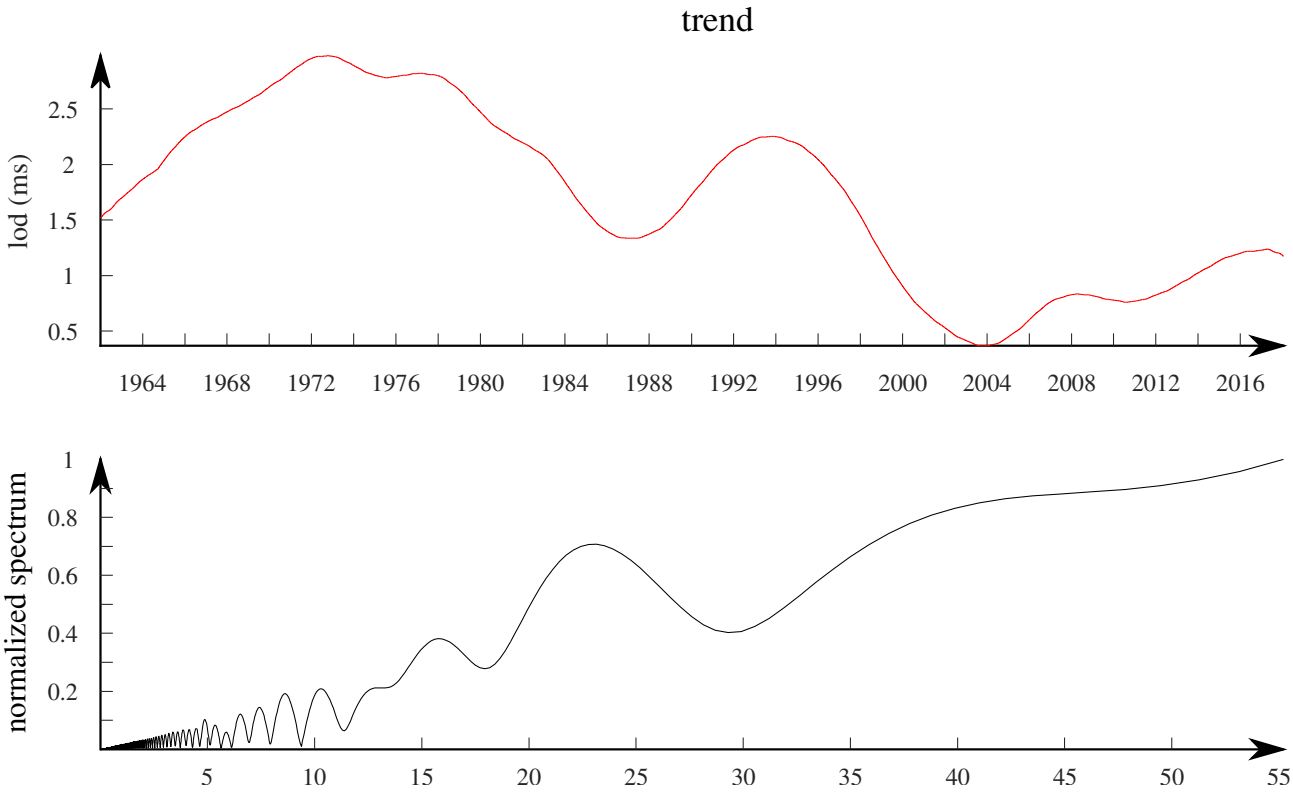
trend
lod (ms)
2.5
2
1.5
1
0.5
1964
1968
1972
1976
1980
1984
1988
1992
1996
2000
2004
2008
2012
2016
normalized spectrum
1
0.8
0.6
0.4
0.2
5
10
15
20
25
30
35
40
45
50
55

Figure 4

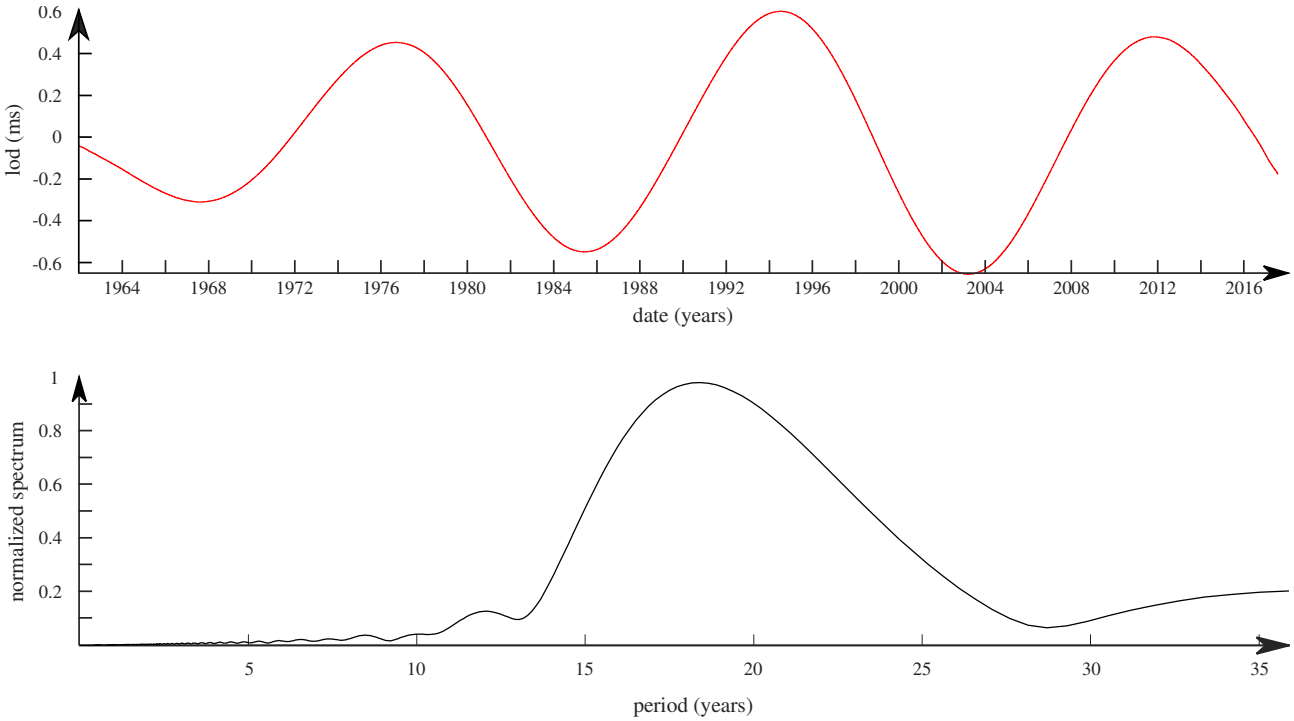
0.6
0.4
0.2
0
-0.2
-0.4
-0.6
lod (ms)
1964
1968
1972
1976
1980
1984
1988
1992
1996
2000
2004
2008
2012
2016
date (years)
1
0.8
0.6
0.4
0.2
normalized spectrum
5
10
15
20
25
30
35
period (years)

Figure 5

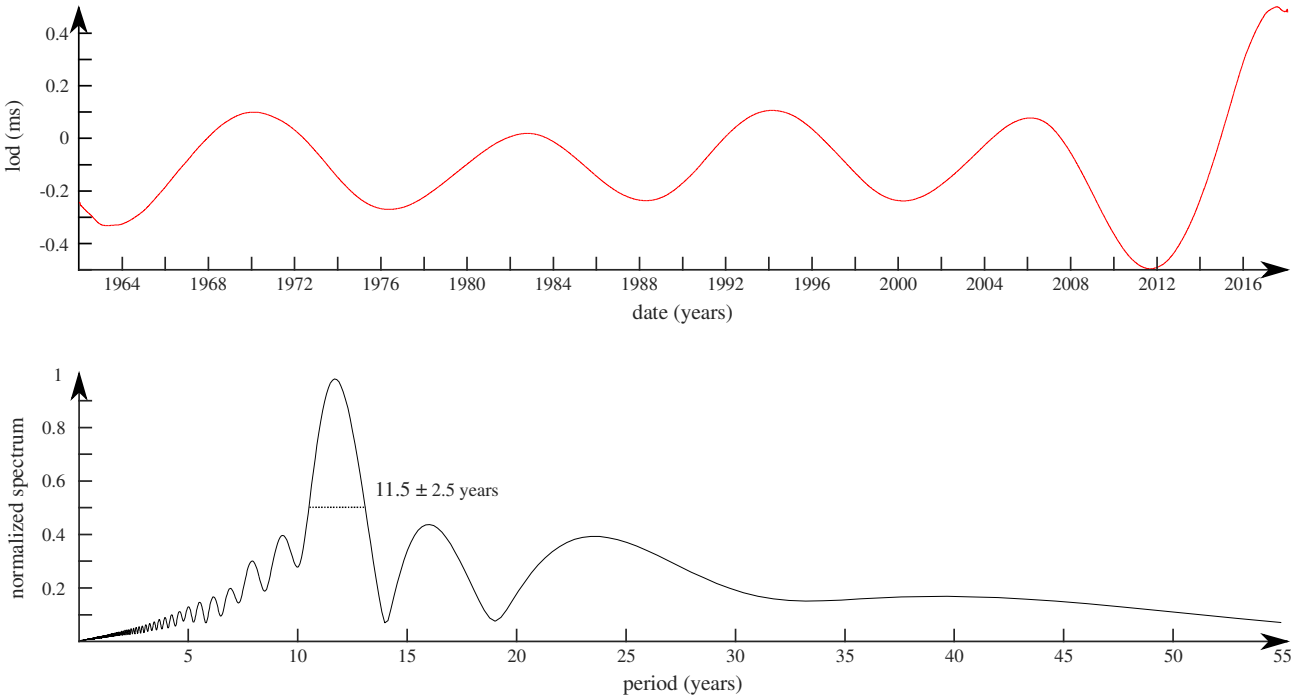
lod (ms)
0.4
0.2
0
-0.2
-0.4
1964
1968
1972
1976
1980
1984
1988
1992
1996
2000
2004
2008
2012
2016
date (years)
normalized spectrum
1
0.8
0.6
0.4
0.2
11.5 ± 2.5 years
5
10
15
20
25
30
35
40
45
50
55
period (years)

Figure 6

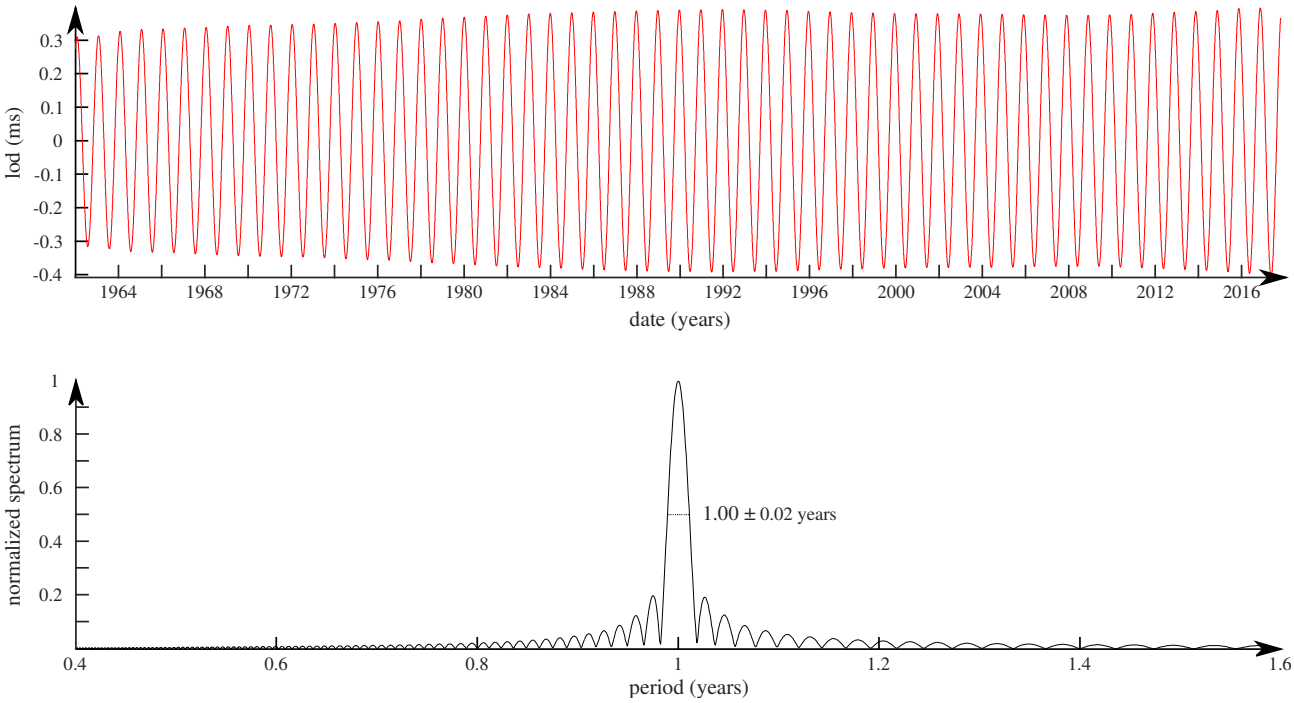
lod (ms)
0.3
0.2
0.1
0
-0.1
-0.2
-0.3
-0.4
1964
1968
1972
1976
1980
1984
1988
1992
1996
2000
2004
2008
2012
2016
date (years)
normalized spectrum
1
0.8
0.6
0.4
0.2
1.00 ± 0.02 years
0.4
0.6
0.8
1
1.2
1.4
1.6
period (years)

Figure 7

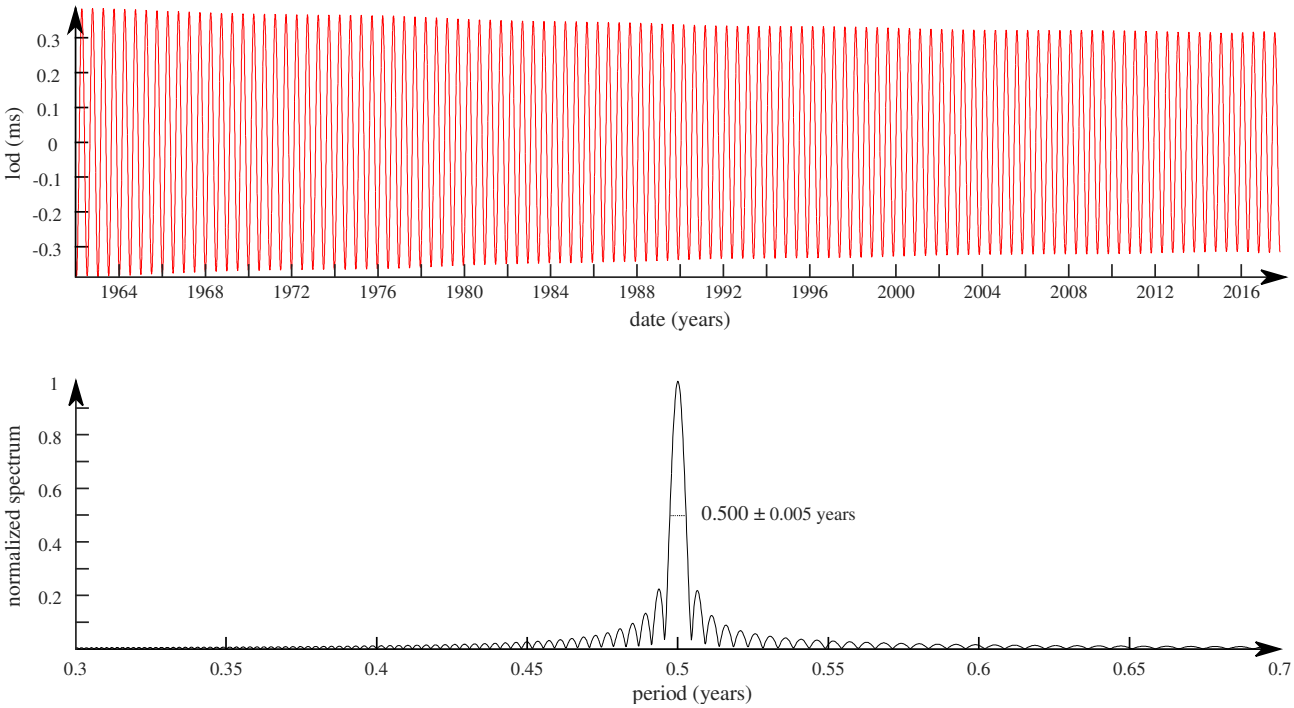
lod (ms)
0.3
0.2
0.1
0
-0.1
-0.2
-0.3
1964
1968
1972
1976
1980
1984
1988
1992
1996
2000
2004
2008
2012
2016
date (years)
normalized spectrum
1
0.8
0.6
0.4
0.2
0.500 ± 0.005 years
0.3
0.35
0.4
0.45
0.5
0.55
0.6
0.65
0.7
period (years)

Figure 8

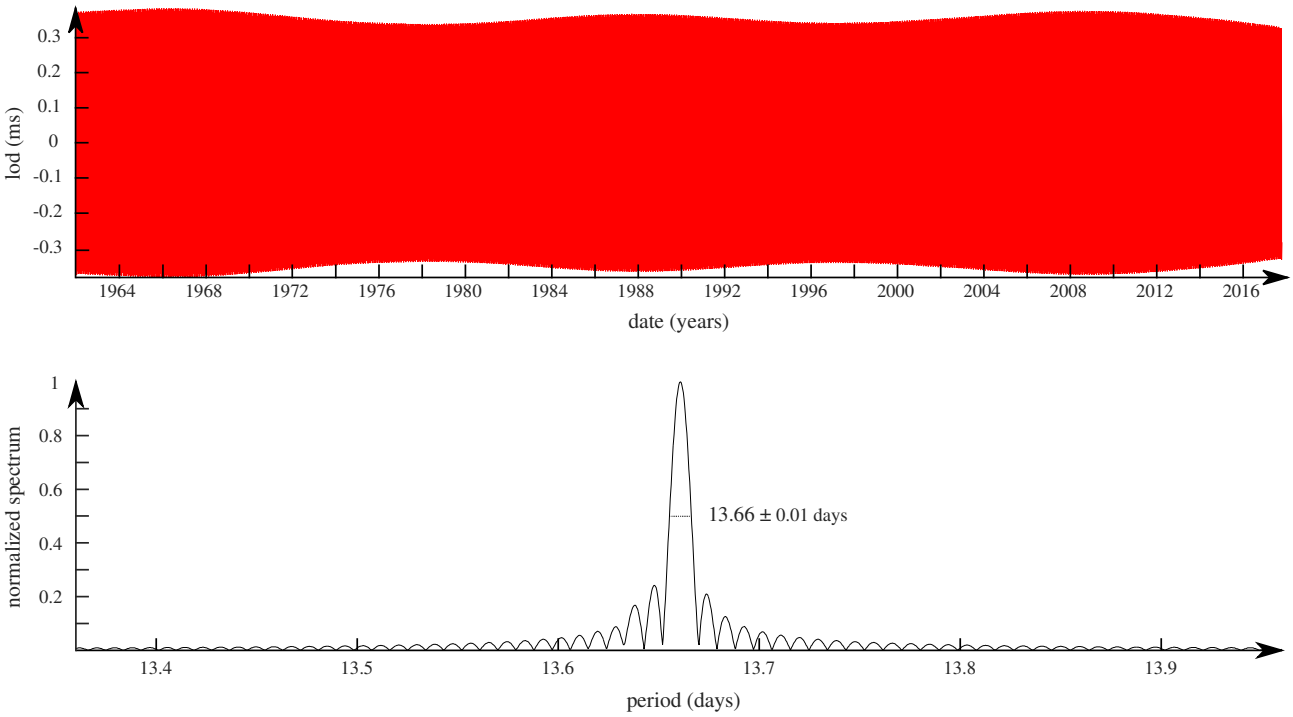
0.3
0.2
0.1
0
-0.1
-0.2
-0.3
lod (ms)
1964
1968
1972
1976
1980
1984
1988
1992
1996
2000
2004
2008
2012
2016
date (years)
1
0.8
0.6
0.4
0.2
normalized spectrum
13.66 ± 0.01 days
13.4
13.5
13.6
13.7
13.8
13.9
period (days)

Figure 9

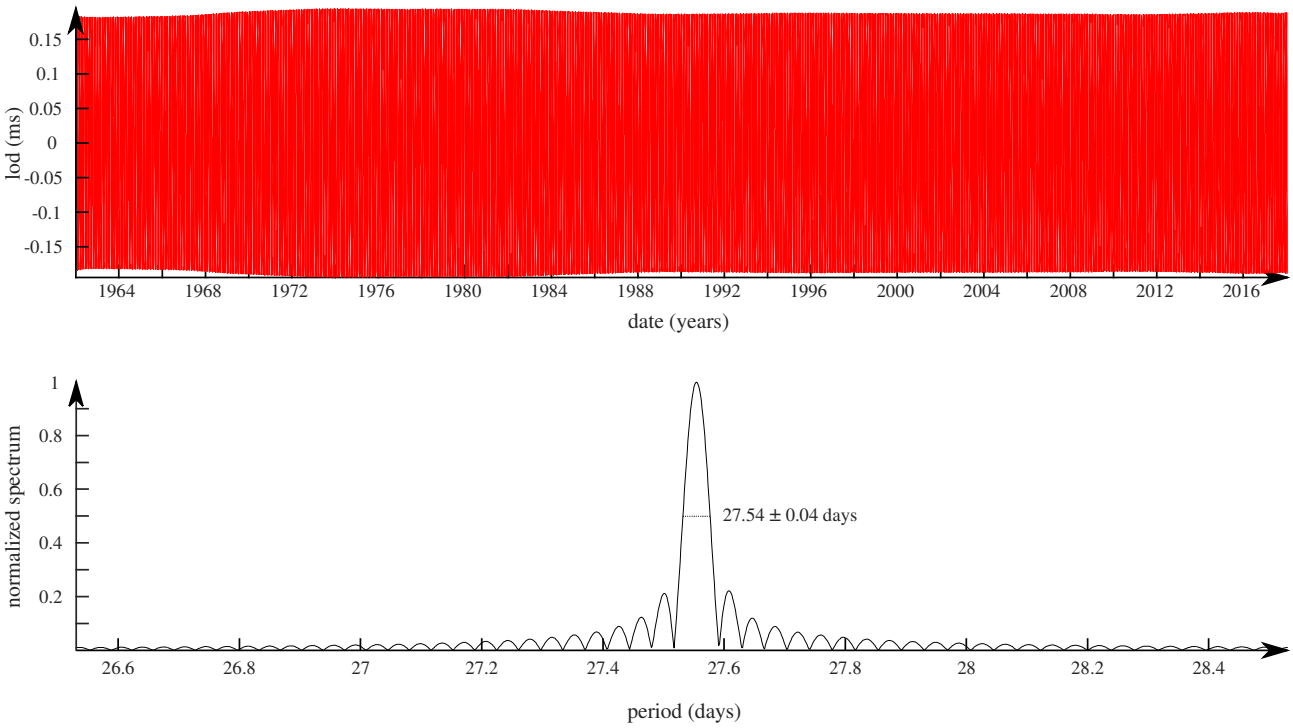
0.15
0.1
0.05
0
-0.05
-0.1
-0.15
lod (ms)
1964
1968
1972
1976
1980
1984
1988
1992
1996
2000
2004
2008
2012
2016
date (years)
1
0.8
0.6
0.4
0.2
normalized spectrum
27.54 ± 0.04 days
26.6
26.8
27
27.2
27.4
27.6
27.8
28
28.2
28.4
period (days)

Figure 10

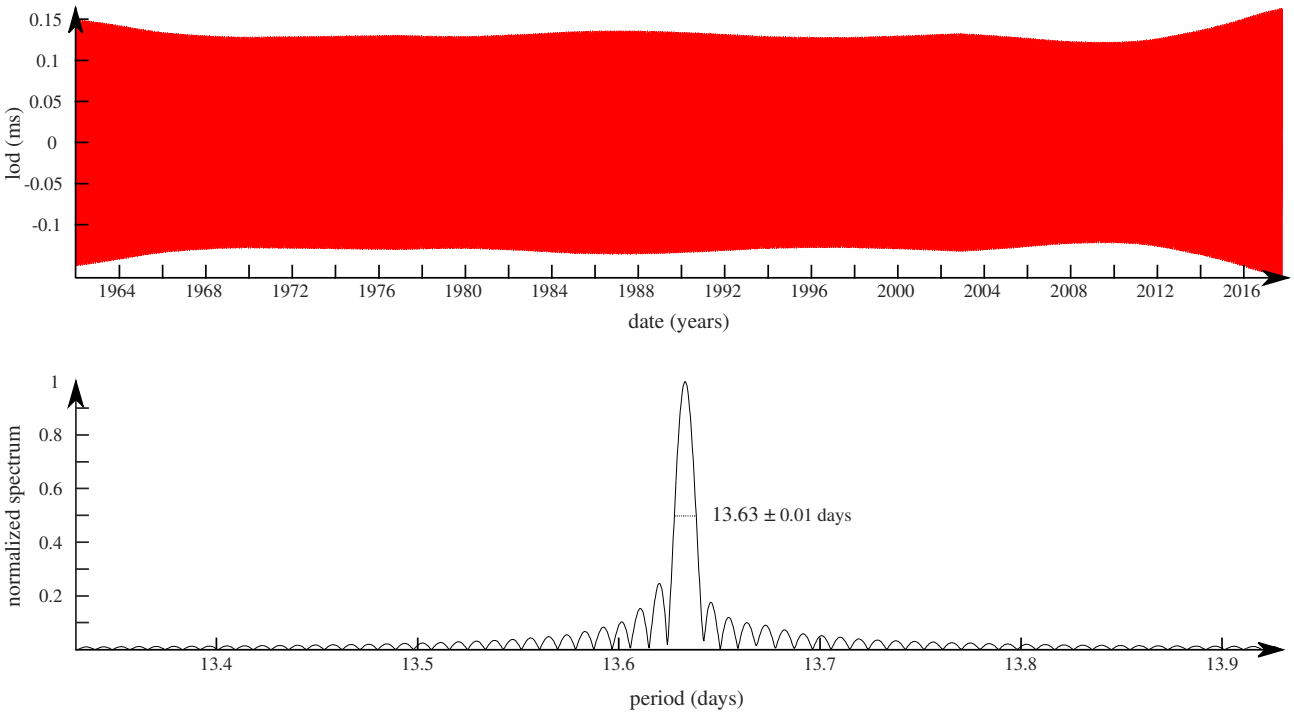
0.15
0.1
0.05
0
-0.05
-0.1
lod (ms)
1964
1968
1972
1976
1980
1984
1988
1992
1996
2000
2004
2008
2012
2016
date (years)
1
0.8
0.6
0.4
0.2
normalized spectrum
13.63 ± 0.01 days
13.4
13.5
13.6
13.7
13.8
13.9
period (days)

Figure 11

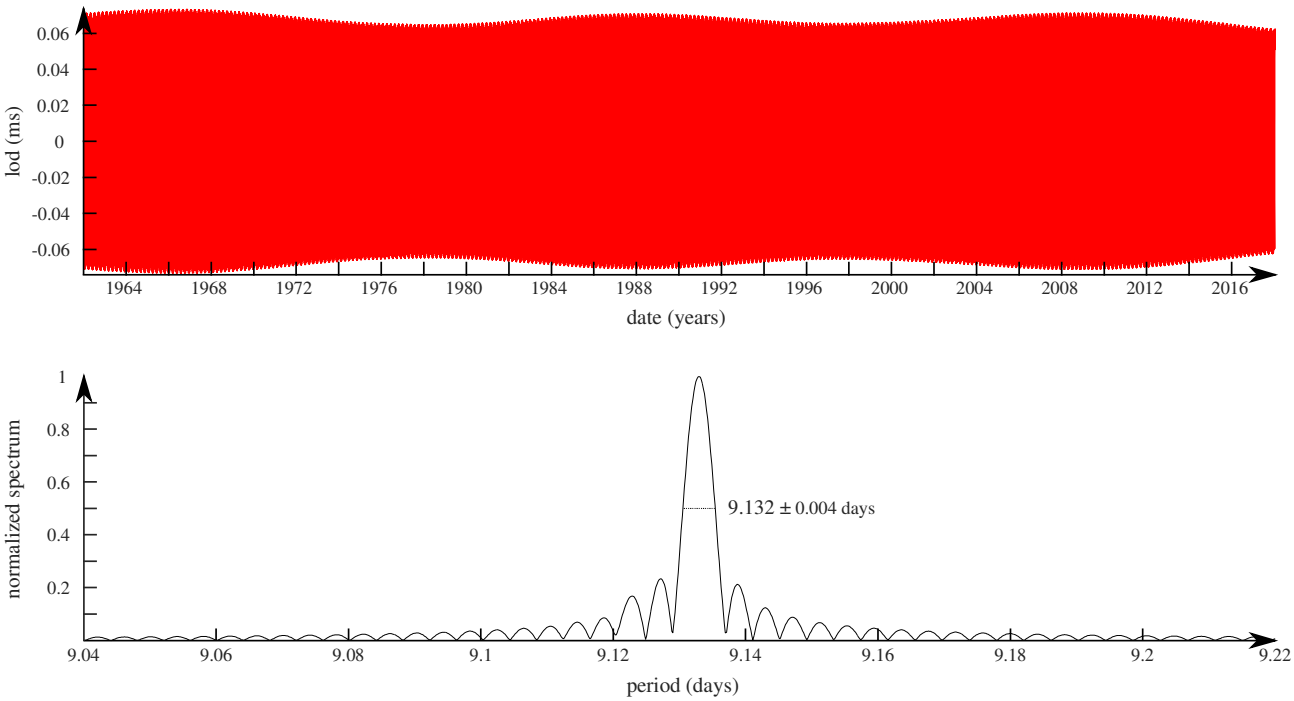
0.06
0.04
0.02
0
-0.02
-0.04
-0.06
lod (ms)
1964
1968
1972
1976
1980
1984
1988
1992
1996
2000
2004
2008
2012
2016
date (years)
1
0.8
0.6
0.4
0.2
normalized spectrum
9.132 ± 0.004 days
9.04
9.06
9.08
9.1
9.12
9.14
9.16
9.18
9.2
9.22
period (days)

Figure 12

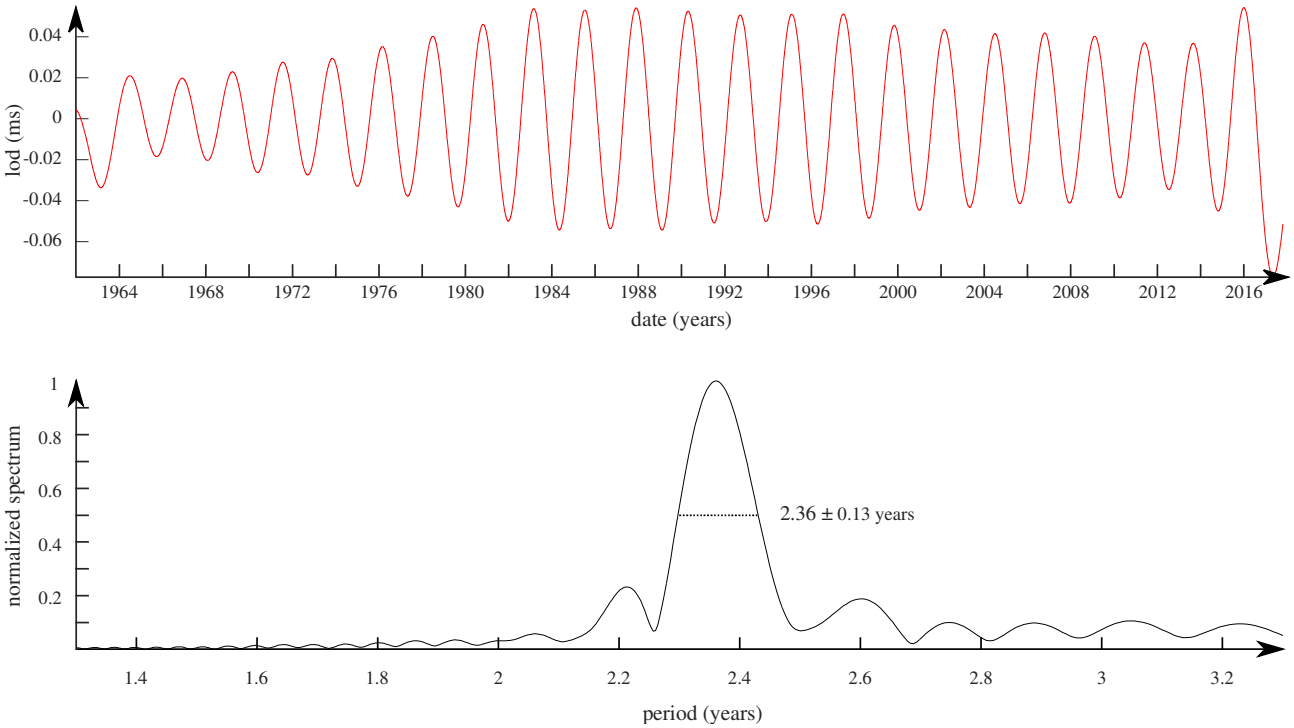
0.04
0.02
0
-0.02
-0.04
-0.06
lod (ms)
1964
1968
1972
1976
1980
1984
1988
1992
1996
2000
2004
2008
2012
2016
date (years)
1
0.8
0.6
0.4
0.2
normalized spectrum
2.36 ± 0.13 years
1.4
1.6
1.8
2
2.2
2.4
2.6
2.8
3
3.2
period (years)

Figure 13

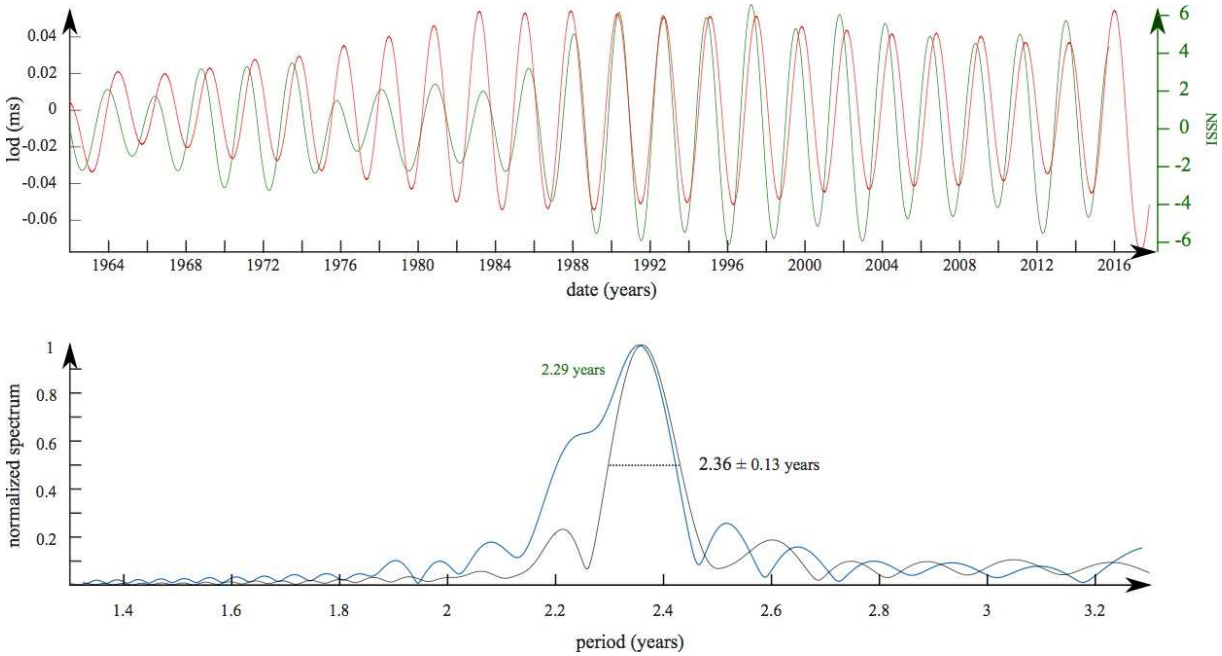
lod (ms)
0.04
0.02
0
-0.02
-0.04
-0.06
ISSN
6
4
2
0
-2
-4
-6
1964
1968
1972
1976
1980
1984
1988
1992
1996
2000
2004
2008
2012
2016
date (years)
normalized spectrum
1
0.8
0.6
0.4
0.2
2.29 years
2.36 ± 0.13 years
1.4
1.6
1.8
2
2.2
2.4
2.6
2.8
3
3.2
period (years)